

Crystallization and preliminary diffraction studies of a truncated form of a novel protease from spores of *Bacillus megaterium*

Karthe Ponnuraj,^a Stephen Kelly,^a Claudio Nessi,^b Peter Setlow^b and Mark J. Jedrzej^{a*}

^aDepartment of Microbiology, University of Alabama at Birmingham, Birmingham, Alabama 35294, USA, and ^bDepartment of Biochemistry, University of Connecticut Health Center, Farmington, Connecticut 06030, USA

Correspondence e-mail: jedrzej@uab.edu

During germination of spores of *Bacillus* species, a novel protease termed GPR initiates the degradation of a group of small acid-soluble spore proteins which protect the dormant spore's DNA from damage. Trypsin digestion of the zymogen of *B. megaterium* GPR removes ~15 kDa from the C-terminal end of the 46 kDa zymogen subunit, leaving a 30 kDa subunit. Single crystals of this truncated form of GPR have been obtained by the vapor-diffusion method using PEG 4000 as a precipitating agent. The crystals belong to the monoclinic space group $P2_1$, with unit-cell parameters $a = 67.99$, $b = 105.34$, $c = 108.63$ Å, $\beta = 95.68^\circ$. The cryofrozen crystals diffract X-rays to about 3.3 Å using synchrotron radiation.

Received 15 July 1999

Accepted 20 October 1999

1. Introduction

Approximately 10–20% of the protein in dormant spores of *Bacillus* species is made up of a group of small acid-soluble spore proteins (SASPs; Setlow, 1988). Some of these SASPs are DNA-binding proteins which saturate the spore DNA and play an important role in protecting spore DNA from damage caused by heat, UV radiation and toxic chemicals (Setlow, 1988, 1995; Setlow & Setlow, 1993). SASPs are degraded to amino acids during spore germination and this degradation is initiated by a sequence-specific enzyme called germination protease (GPR; Setlow, 1988). This tetrameric protease ($M_w = 160$ – 185 kDa) exhibits no obvious amino-acid sequence similarity to any of the known classes of protease, and chemical-modification studies, metal-ion analysis, site-directed mutagenesis of Ser and Cys residues and the use of protease inhibitors have shown that GPR is not an aspartic, metallo-, serine or cysteine protease (Nessi *et al.*, 1998). This suggests that GPR may be a novel protease.

During sporulation, GPR is synthesized as an inactive zymogen (termed P_{46}) in the developing forespore, approximately in parallel with synthesis of its SASP substrates (Setlow, 1976, 1988; Sanchez-Salas & Setlow, 1993). Approximately 2 h later in sporulation P_{46} autoprocesses to a smaller protein (termed P_{41}) through removal of 15 (*B. megaterium*) or 16 (*B. subtilis*) N-terminal residues (Nessi *et al.*, 1998). Although P_{41} is active *in vitro*, this protein does not degrade SASP in the developing or dormant spore, probably because of the decreased pH and hydration level both in the forespore at the time of P_{46} to P_{41} conver-

sion and in the dormant spore (Setlow, 1988, 1994; Sanchez-Salas & Setlow, 1993). However, when spore germination commences and the elevation of spore core pH and hydration take place, P_{41} becomes active *in vivo* and initiates rapid SASP degradation. This SASP degradation leads to uncoating of the spore's DNA, facilitating subsequent DNA transcription, and the amino acids produced are used for protein synthesis during further development of the germinated spore (Setlow, 1988; Illades-Aguiar & Setlow, 1994b).

While much is known about the changes in GPR upon conversion of P_{46} to P_{41} and how this process is regulated, a number of key questions remain unanswered including why P_{46} is inactive, how P_{46} is activated, what the catalytic mechanism of P_{41} is and, in particular, what the changes in GPR structure upon conversion of P_{46} to P_{41} are. Circular dichroism spectroscopic studies (Nessi *et al.*, 1998) have shown that there is no major difference between the secondary structures of P_{46} and P_{41} . However, analysis of the reactivity of the protein's single sulfhydryl group (Illades-Aguiar & Setlow, 1994a) as well as thermal unfolding studies (Nessi *et al.*, 1998) suggest that there is a difference between the tertiary structures of P_{46} and P_{41} . Consequently, it appears likely that detailed structural analysis of P_{46} and P_{41} will further our understanding of the mechanism of the P_{46} to P_{41} conversion, the reason for the inactivity of P_{46} and the mechanism of P_{41} catalysis.

In addition to GPR, many other proteases exist in both zymogen and active forms and X-ray crystallography has been used to determine the structures of the zymogen and active forms of many such proteases (Khan & James,

Table 1
X-ray diffraction data-collection statistics for *B. megaterium* P₃₀ crystals.

The data set was collected as described in §2.

Resolution shell (Å)	Number of unique reflections	$R_{\text{merge}}^{\dagger}$	$I/\sigma(I)$	Completeness (%)
50.00–7.64	1708	0.071	23.9	91.0
7.64–6.07	1779	0.080	22.8	95.3
6.07–5.30	1779	0.090	18.3	95.7
5.30–4.82	1757	0.092	17.0	95.2
4.82–4.47	1770	0.088	16.4	95.5
4.47–4.21	1743	0.121	11.6	95.0
4.21–4.00	1754	0.184	7.1	95.3
4.00–3.82	1749	0.293	4.3	95.5
3.82–3.68	1766	0.308	4.2	95.3
3.68–3.55	1743	0.378	3.4	95.1
50.00–3.55	17548	0.111	12.1	94.8

$\dagger R_{\text{merge}} = \sum |I - \langle I \rangle| / \sum I$, where I is the intensity of an individual measurement and $\langle I \rangle$ is the average intensity from multiple observations.

1998). Since analysis of these structures has provided tremendous insight into the bases for both zymogen inactivity and activation, we have initiated X-ray crystallographic analysis of the structures of both P₄₆ and P₄₁ and have previously reported evidence for structural differences between P₄₆ and P₄₁ based on differences in their crystallization (Ponnuraj *et al.*, 1998).

To investigate further the structure of P₄₆ and P₄₁ and to isolate stable domains of these proteins that might give high-quality crystals, both P₄₆ and P₄₁ from *B. megaterium* were digested with trypsin (Nessi *et al.*, 1998). Trypsin rapidly converted P₄₆ to a 30 kDa species (termed P₃₀) that was resistant to further digestion and encompassed GPR residues 3–268. Not only did P₃₀ remain enzymatically inactive, it also retained the ability to autoprocess properly to a smaller form that was active in SASP cleavage. In contrast, P₄₁ was degraded by trypsin to multiple fragments of less than 10 kDa, none of which retained catalytic activity. While the results of these studies

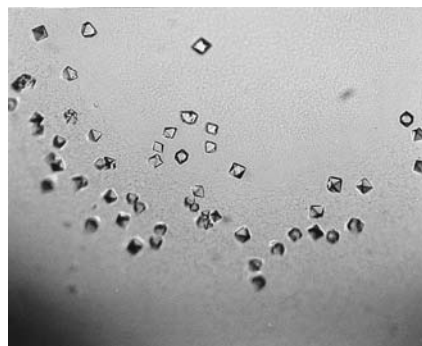


Figure 1
Crystals of *B. megaterium* P₃₀ grown at 295 K from PEG 4000 and 0.1 M Tris-HCl (pH 8.3) as described in §2.

further highlighted the differences in the tertiary structures of P₄₆ and P₄₁, they also showed that loss of ~15 kDa from the C-terminus of P₄₆ destroyed neither the catalytic nor the autoprocessing activity of the enzyme. This further indicates that the residues essential for zymogen inactivity and autoprocessing as well as P₄₁ catalysis reside in the N-terminal 70% of the protein. This latter conclusion prompted us to initiate X-ray crystallographic studies with P₃₀, in the hope that the eventual comparison of the structures of P₄₆ and P₃₀ (and with the possibility of higher quality crystals of the latter protein) might give a clearer picture of the active site and catalytic mechanism of GPR. In this communication, we report the crystallization and preliminary diffraction analysis of P₃₀ crystals.

2. Experimental

The expression and purification of *B. megaterium* P₄₆ was carried out as reported previously (Nessi *et al.*, 1998). For trypsin digestion of P₄₆, 1.0 ml of 10 mg ml⁻¹ P₄₆ was incubated for 3 h at 310 K in 50 mM Tris-HCl (pH 7.4), 20% glycerol, 5 mM CaCl₂ with 10 µl of 1 mg ml⁻¹ tosylsulfonyl phenylalanyl chloromethyl ketone (TPCK) treated trypsin (Worthington Biochemical Corp., Lakewood, NJ, USA) as described (Nessi *et al.*, 1998). The degradation reaction was stopped by the addition of 0.5 mg of soybean trypsin inhibitor bound to DITC glass beads (Sigma Chemical, St Louis, MO, USA). After further incubation for 30 min at 310 K, the sample was centrifuged for 10 min at 2000g to remove the trypsin and trypsin inhibitor; all subsequent steps were performed at 277–283 K. The supernatant fluid was run on a Superdex 200 10/30 gel-filtration column (Amersham Pharmacia Biotech, Piscataway, NJ, USA) equilibrated with buffer A (10 mM Tris-HCl pH 7.4, 5 mM CaCl₂, 10% glycerol) containing 100 mM NaCl. The fractions containing P₃₀ were pooled and loaded on a Mono-Q 5/5 column (Amersham Pharmacia Biotech, Piscataway, NJ, USA) equilibrated with buffer A containing 100 mM NaCl and were eluted with a linear gradient of 100–500 mM NaCl in buffer A. For crystallization, P₃₀ was concentrated to 10 mg ml⁻¹ in buffer A containing 250 mM NaCl using Centricon-30 concentrators (Amicon, Beverly, MA, USA). Crystallization trials were performed

using the hanging-drop vapor-diffusion method (McPherson, 1990).

An initial crystallization screening at room temperature with Hampton Research crystallization kits I and II (Hampton Research, Laguna Hills, CA, USA) revealed small crystals using PEG 4000 as precipitant. Optimized crystallization conditions consisted of mixing 2 µl of protein and 2 µl of reservoir solution containing 32% PEG 4000 with 0.1 M Tris-HCl (pH 8.3) at 295 K. Well formed crystals of P₃₀ appeared within 4 d and reached dimensions of 0.2 × 0.2 × 0.15 mm (Fig. 1). Preliminary X-ray diffraction studies were carried out at room temperature on an R-AXIS II image-plate system using a Rigaku RU-300 X-ray generator with Cu Kα radiation (Molecular Structure Corp., The Woodlands, TX, USA) operating at 50 kV and 100 mA. The crystals were sensitive to radiation damage and diffracted only to about 5 Å resolution. In order to avoid radiation damage, crystals were loop-mounted in a cryoprotecting solution containing 5% glycerol and the crystal mother liquor and maintained frozen at 103 K. Because of the limited resolution and small size of the crystals, synchrotron radiation was used for X-ray diffraction data collection.

3. Conclusions

Native reflection intensities were measured at beamline X25 at the National Synchrotron Light Source of the Brookhaven National Laboratory using a wavelength of 1.15 Å and the Brandeis 2 × 2 CCD-based detector on the hybrid Nonius goniometer. The crystals diffracted to about 3.3 Å with only weak reflections present beyond 3.55 Å. The unit cell was determined using the autoindexing procedures of DENZO (Otwinowski & Minor, 1997) to be monoclinic with unit-cell parameters $a = 67.99$, $b = 105.34$, $c = 108.63$ Å, $\beta = 95.68^\circ$. Examination of systematic absences indicated space group $P2_1$. Assuming five or six molecules in the asymmetric unit, the crystal volume per protein mass V_m (Matthews, 1968) was 2.62 or 2.18 Å³ Da⁻¹, respectively, with both values falling in the normal range for protein crystals. With five or six molecules in the asymmetric unit, the solvent content was determined to be 53 or 43%, respectively.

The oscillation images, with a 1.0° oscillation range and a 30 s exposure to X-rays, were analyzed and indexed with DENZO (Otwinowski & Minor, 1997) and scaled with SCALEPACK (Otwinowski & Minor, 1997). A complete data set was collected on

cryofrozen crystals maintained at 103 K. Processing of 49 173 measured reflections led to 17 548 unique reflections with an R_{merge} of 11.1%. The data were 94.8% complete in the resolution range 50.0–3.55 Å, with an average $I/\sigma(I)$ of 12.1. Some statistics of the data collection are shown in Table 1. Although the completeness is more than 90% in the resolution range 3.55–3.3 Å, R_{merge} was greater than 65% and $I/\sigma(I)$ was around 1.0. Therefore, this shell was discarded in the final processing of the data.

As we have recently been successful in determining the *B. megaterium* P₄₆ structure by the multiwavelength anomalous dispersion technique using the selenomethionyl derivative of P₄₆ (Ponnuraj *et al.*, in preparation), we plan to solve the structure of P₃₀ by the molecular-replacement method using a truncated P₄₆ model as a probe. The knowledge of the P₃₀ structure and the comparison of this structure with that of P₄₆

and ultimately with that of P₄₁ will certainly shed light on how the N-terminal two-thirds of GPR is required for the catalytic activity of this protease, the maintenance of P₃₀ and P₄₆ in an inactive state and the mechanism of autoprocessing P₃₀ and P₄₆ into active enzymes.

Diffraction data for this study were collected at Brookhaven National Laboratory in the Biology Department's single-crystal diffraction facility at beamline X25 in the National Synchrotron Light Source. This facility is supported by the United States Department of Energy Offices of Health and Environmental Research and of Basic Energy Sciences under prime contract DE-AC02-98CH10886, by the National Science Foundation and by National Institutes of Health Grant 1P41 RR12408-01A1. The work in the Setlow laboratory was supported by a grant from the Army Research Office (ARO).

References

- Illades-Aguilar, B. & Setlow, P. (1994a). *J. Bacteriol.* **176**, 5571–5573.
- Illades-Aguilar, B. & Setlow, P. (1994b). *J. Bacteriol.* **176**, 7032–7037.
- Khan, A. R. & James, M. N. G. (1998). *Protein Sci.* **7**, 815–836.
- McPherson, A. (1990). *Eur. J. Biochem.* **189**, 1–23.
- Matthews, B. W. (1968). *J. Mol. Biol.* **33**, 491–497.
- Nessi, C., Jedrzejewski, M. J. & Setlow, P. (1998). *J. Bacteriol.* **180**, 5077–5084.
- Otwinowski, Z. & Minor, W. (1997). *Methods Enzymol.* **276**, 307–326.
- Ponnuraj, K., Nessi, C., Setlow, P. & Jedrzejewski, M. J. (1998). *J. Struct. Biol.* **125**, 19–24.
- Sanchez-Salas, J. L. & Setlow, P. (1993). *J. Bacteriol.* **175**, 2568–2577.
- Setlow, B. & Setlow, P. (1993). *Appl. Environ. Microbiol.* **59**, 3418–3423.
- Setlow, P. (1976). *J. Biol. Chem.* **251**, 7853–7862.
- Setlow, P. (1988). *Annu. Rev. Microbiol.* **42**, 319–338.
- Setlow, P. (1994). *J. Appl. Bacteriol.* **76**, 49S–60S.
- Setlow, P. (1995). *Annu. Rev. Microbiol.* **49**, 29–54.